Amrit Raj Ghosh,[1] Roopkatha Bhattacharya,[1] Shamik Bhattacharya,[1] Titli Nargis,[2] Oindrila Rahaman,[1] Pritam Duttagupta,[1] Deblina Raychaudhuri,[1] Chinky Shiu Chen Liu,[1] Shounak Roy,[1] Parasar Ghosh,[3] Shashi Khanna,[4] Tamonas Chaudhuri,[4] Om Tantia,[4] Stefan Haak,[5] Santu Bandyopadhyay,[1] Satinath Mukhopadhyay,[6] Partha Chakrabarti,[2] and Dipyaman Ganguly[1]

Adipose Recruitment and Activation of Plasmacytoid Dendritic Cells Fuel Metaflammation

Diabetes 2016;65:3440–3452 | DOI: 10.2337/db16-0331

In obese individuals, visceral adipose tissue (VAT) is the seat of chronic low-grade inflammation (metaflammation), but the mechanistic link between increased adiposity and metaflammation largely remains unclear. In obese individuals, deregulation of a specific adipokine, chemerin, contributes to innate initiation of metaflammation by recruiting circulating plasmacytoid dendritic cells (pDCs) into VAT through chemokine-like receptor 1 (CMKLR1). Adipose tissue–derived high-mobility group B1 (HMGB1) protein activates Toll-like receptor 9 (TLR9) in the adipose-recruited pDCs by transporting extracellular DNA through receptor for advanced glycation end products (RAGE) and induces production of type I interferons (IFNs). Type I IFNs in turn help in proinflammatory polarization of adipose-resident macrophages. IFN signature gene expression in VAT correlates with both adipose tissue and systemic insulin resistance (IR) in obese individuals, which is represented by ADIPO-IR and HOMA2-IR, respectively, and defines two subgroups with different susceptibility to IR. Thus, this study reveals a pathway that drives adipose tissue inflammation and consequent IR in obesity.

Obesity and associated metabolic disorders are major health problems worldwide. Studies over the past decade have established that visceral adipose tissue (VAT) in obese individuals harbors chronic low-grade inflammation, termed metaflammation, involving myriad innate and adaptive immune cell subsets (1–3). Interest in mechanisms of metaflammation grew after discovery of resident macrophages in VAT of obese individuals (4).

The chemokine-receptor axis CCL2-CCR2 has been implicated in the recruitment of monocyte-derived macrophages into adipose tissue (5,6). In obese VAT, as opposed to lean VAT, the resident macrophages show a classically activated proinflammatory M1 phenotype rather than the so-called alternatively activated anti-inflammatory M2 phenotype (2). Although $CCR2^{+}$ macrophages have been shown to be recruited in response to CCL2 expressed in obese VAT, no evidence points to selective recruitment of M1 macrophages in response to CCL2. One study shows that CCL2 promotes an M2 phenotype (7). Thus, the switch in the macrophage phenotype in response to hyperadiposity cannot be explained by the CCL2-CCR2 axis. Therefore, the potential mediators for the M2-to-M1 switch are probably induced in obese VAT in situ.

One of the proposed candidates is circulating free fatty acid (FFA), which might induce proinflammatory cytokine production from adipocytes through Toll-like receptor 4 (TLR4) (8). These adipose-derived cytokines in turn can affect the macrophage phenotypic switch in situ as well as systemic insulin resistance (IR) (9). Fetuin-A, a

[1]Division of Cancer Biology and Inflammatory Disorders, Council of Scientific and Industrial Research-Indian Institute of Chemical Biology, Kolkata, India
[2]Division of Cell Biology and Physiology, Council of Scientific and Industrial Research-Indian Institute of Chemical Biology, Kolkata, India
[3]Department of Rheumatology, Institute of Postgraduate Medical Education and Research, Kolkata, India
[4]ILS Hospitals, Kolkata, India
[5]Zentrum Allergie und Umwelt, Technical University of Munich and Helmholtz Centre Munich, Munich, Germany
[6]Department of Endocrinology, Institute of Postgraduate Medical Education and Research, Kolkata, India

Corresponding author: Dipyaman Ganguly, dipyaman@iicb.res.in.

Received 11 March 2016 and accepted 19 August 2016.

This article contains Supplementary Data online at http://diabetes.diabetesjournals.org/lookup/suppl/doi:10.2337/db16-0331/-/DC1.

fatty acid–binding glycoprotein secreted from the liver, has been implicated in mediating TLR4 activation by FFAs (10). Nevertheless, the mechanistic link between metabolic deregulation associated with increased adiposity and innate immune initiation of metaflammation remains largely unclear. A major adipose-intrinsic deregulation in obesity is change in adipokine expression levels. An imbalance between two such adipokines, leptin and adiponectin, has been found to be instrumental for the metabolic derangements associated with obesity (11). Chemerin (expressed by tazarotene-induced gene 2 [TIG2]) is another such adipokine that regulates adipocyte development, differentiation, and metabolic function (12). Chemerin expression in adipocytes is increased with abundance of FFAs (13); accordingly, its systemic level has been found to be elevated in obese patients with metabolic syndrome (14,15). Moreover genetic deficiency of chemokine-like receptor 1 (CMKLR1), the cognate receptor for chemerin, in mice protects them from high-fat diet (HFD)–induced IR (14). Of note, chemerin also acts as a chemokine for immune cells acting through CMKLR1, specifically plasmacytoid dendritic cells (pDCs) (16), the major type I interferon (IFN)–producing cells in the body. In autoimmune contexts, like psoriasis, chemerin has been shown to recruit pDCs in tissues and initiate the cascade of autoreactive inflammation through type I IFNs (17–19).

We wondered whether adipose tissue–derived chemerin is involved in linking hyperadiposity to initiation of metaflammation by playing a similar chemotactic function in obesity as well. We collected VAT samples from obese individuals, and by means of whole-tissue gene expression, adipose explant culture, and cell culture studies, we unraveled a role of chemerin-recruited pDCs and type I IFNs in the initiation of metaflammation.

RESEARCH DESIGN AND METHODS

Patients and Tissue Samples

We recruited 83 obese and 29 lean individuals who were undergoing bariatric surgery or other abdominal surgeries, respectively, at the ILS Hospitals, Kolkata, India. Relevant characteristics of the recruited patients are shown in Table 1. Greater omental adipose tissue samples from all obese individuals and 11 lean individuals and peripheral blood samples were collected after written informed consent per recommendations of the institutional review boards of all participating institutions.

RNA Isolation and Quantitative Real-Time PCR

Total RNA was isolated from both in vitro–cultured and ex vivo–sorted macrophages and VAT using TRIzol reagent (Life Technologies, Frederick, MD). cDNA was synthesized with Superscript III (Thermo Fisher Scientific, Waltham, MA) and assayed for expression of indicated genes by an Applied Biosystems 7500 Fast Real-Time PCR using SYBR Green Master Mix (Roche, Basel, Switzerland). The primers are listed in Supplementary Table 1.

Isolation of Stromal Vascular Fraction From VAT

Major macroscopic blood vessels were removed by dissection from the VAT samples followed by wash with PBS (three changes) and digestion in PBS supplemented with 0.075% collagenase I, 1% BSA, and 1% HEPES at 37°C. Stromal vascular fraction (SVF) was obtained by centrifugation of the digested VAT at 300*g* for 10 min followed by

Table 1—Anthropometric and biochemical parameters of the recruited individuals

	Data available		Values	
Parameters	Obese	Lean	Obese	Lean
Total	83	29	—	—
Female	49	8	—	—
Male	34	21	—	—
Age (years)	83	29	41.2857 ± 12.0866	44.7241 ± 11.4483
BMI (kg/m^2)	76	29	43.9388 ± 7.46692	25.07037 ± 3.09401
VAT samples	83	11	—	—
Plasma samples	72	28	—	—
Fasting blood glucose (mg/dL)	78	29	128.7462 ± 59.1401	103.5862 ± 19.4082
Fasting plasma insulin (μU/mL)	63	0	25.3906 ± 14.2685	NA
HbA_{1c} (%)	63	20	7.15873 ± 1.719118	5.445 ± 0.551052
HbA_{1c} (mmol/mol)	63	20	57.23809 ± 21.8216	35.9 ± 6.086223
Plasma FFA (μmol/L)	64	0	296.6826 ± 114.731	NA
Plasma chemerin (ng/mL)	72	28	75.2466 ± 23.2116	15.4 ± 18.6437
ADIPO-IR	64	0	49.198 ± 37.125	NA
HOMA2-IR	63	0	3.5211± 2.0888	NA

Data are *n* and mean ± SD. NA, not available.

passage through a 100-μm cell strainer (SPL Life Sciences, Gyeonggi-do, Korea).

Flow Cytometric Analysis and Sorting

$CD123^+CLEC4c^+$ pDCs in the SVFs from VAT samples were enumerated with the following fluorophore-tagged antibodies: CD45 phycoerythrin (PE) (BD Biosciences, San Diego, CA) and CD3 fluorescein isothiocyanate (FITC), CD8 peridinin-chlorophyll-protein (PerCP), CLEC4c allophycocyanin (APC), and CD123 eFlour450 (eBioscience, Santa Clara, CA). To assess surface phenotype of in vitro–generated macrophages, we used anti-human CD14 PerCP, CD11b BV421, CD206 FITC, and CD86 APC (BD Biosciences). Macrophage subsets in the SVF from VAT samples (n = 11) were enumerated using CD3 PerCP and CD163 APC (eBioscience) and CD45-PE, CD11b FITC, and CD11c PE Cy7 (BD Biosciences) to identify M1- ($CD11b^+CD11c^+$) and M2- ($CD11b^+CD163^+$) polarized macrophages by flow cytometry. In some cases (n = 7), the M1 and M2 subsets were sorted on a BD FACS Aria cell sorter for subsequent gene expression studies.

Adipose Tissue Sectioning and Staining

Adipose tissue samples were cryosectioned (15-μm thick slices) in a Leica CM1950 cryotome using Shandon cryomatrix and stained with PE-conjugated BDCA4 antibody (Miltenyi Biotec, Bergisch Gladbach, Germany). DAPI-counterstained sections were mounted with VECTASHIELD (Vector Laboratories, Burlingame, CA) and 200× images were acquired on an EVOS FL fluorescence microscope (Thermo Fisher Scientific).

pDC Isolation and Culture

pDCs were isolated from peripheral blood mononuclear cells by magnetic immunoselection using anti-BDCA4 microbeads (Miltenyi Biotec). Isolated pDCs were cultured in complete RPMI medium (or as indicated) in 96-well U-bottom plates.

Adipose Explant Culture

VAT samples were collected in PBS supplemented with 1% Gibco antibiotic-antimycotic solution (Thermo Fisher Scientific). Minced pieces of tissue were weighed and cultured in complete Gibco RPMI medium. Supernatant (adipose explant culture supernatant [AEC-sup]) was collected from the culture at 1, 7, 14, 24, and 36 h and then cryostored.

pDC Migration Assay

Purified pDCs were cultured for 1 h in RPMI medium with 2% FBS (migration medium) followed by incubation for 15 min in the presence of control antibody (rat IgG2a 1 μg/mL; eBioscience), anti-CMKLR1 antibody (1 μg/mL; eBioscience), or just the migration medium. Then 50×10^3 pDCs in 100 μL was added to the top transwell inserts, and either 600 μL of AEC-sup or control medium was added to the bottom chambers. After 5 h, the plate was kept on ice for 15 min, and the number of migrating cells was counted. In some experiments, purified recombinant human chemerin (10 ng/mL; R&D Systems, Minneapolis, MN) were used to drive pDC migration in the presence of the anti-CMKLR1 antibody or control antibody as described.

Reporter Assays

Human embryonic kidney (HEK) cells (70,000 cells/200 μL) expressing human TLR9 along with a nuclear factor κB (NF-κB) promoter–driven secreted embryonic alkaline phosphatase (SEAP) reporter (InvivoGen, San Diego, CA) were used for assessing TLR9 activation by the AEC-sups. Twenty-five percent of the total volume of AEC-sup or control medium was used for the assays, and the SEAP activity was assessed using QUANTI-Blue detection media (InvivoGen).

pDC Stimulation With AEC-sups

AEC-sups were added to pDC cultures to check for type I IFN induction. To deplete adipose explant supernatants of DNA molecules, the AEC-sups were treated with 200 units/mL DNase (Thermo Fisher Scientific) for 1 h at 37°C before addition to pDC cultures. In some experiments, RAGE receptors were blocked on pDCs using 1 μg/mL anti-human RAGE goat polyclonal antibody (R&D Systems) before adding the AEC-sups. To deplete the HMGB1-bound TLR9 ligands, AEC-sups were added with either 5 μg/mL anti-HMGB1 monoclonal antibody (R&D Systems), control antibody, or none (mock depletion) and then added to the tubes containing protein G magnetic beads (Merck Millipore, Danvers, MA). After incubation for 12 h, the antibody-bound beads were removed by using a Magna rack. Following this, the mock and antibody-depleted supernatants were added to freshly isolated pDCs.

ELISA

ELISA was used to detect and measure IFN-α (Mabtech, Nacka Strand, Sweden) in the supernatants obtained from pDC cultures, tumor necrosis factor α (TNF-α) in the supernatant of macrophage culture (Mabtech), chemerin (Merck Millipore) in AEC-sups, and insulin (Merck Millipore) in plasma samples. ELISAs were performed according to the respective manufacturer's protocol. FFA estimation was done for the plasma samples by using a fluorometric assay kit (Cayman Chemical, Ann Arbor, MI).

RNA Interference

Knockdown of TLR9 expression in freshly isolated pDCs was done with small interfering RNA (siRNA) using nucleofection according to the manufacturer's protocol (Amaxa 4D-Nucleofector Kit; Lonza, Koln, Germany). pDCs (5×10^5) were resuspended in 100 μL of supplemented P3 nucleofection buffer. Control (MISSION esiRNA-targeting EGFP; Sigma-Aldrich, Haverhill, MA) or human TLR9-specific siRNA (sequence: GACCUCUAU CUGCACUUCUdTdT) (Eurogentec, Liège, Belgium) was delivered by using the program FF168. After 18 h of culture in complete RPMI medium, cells were harvested and plated in a 96-well U-bottom plate and treated as indicated.

Macrophage Culture

Peripheral blood CD14$^+$ monocytes were isolated by magnetic immunoselection from healthy peripheral blood mononuclear cells and differentiated to macrophages by culturing in the presence of recombinant human macrophage colony-stimulating factor (M-CSF) (500 units/mL; R&D Systems) in 24-well plates. Forty-eight hours later, recombinant human interleukin-4 (IL-4) (20 ng/mL; Tonbo Biosciences, San Diego, CA) was added to the macrophages to allow polarization to the M2 phenotype and incubated for an additional 48 h (except control wells). Following this, recombinant human IFN-α (PBL Interferon Source, Piscataway, NJ) was added in indicated concentrations (10, 100, and 1,000 units/mL). Cultured macrophages and their supernatants were then harvested and processed after 48 h for further studies. In some experiments, in vitro–generated M2 macrophages (10×10^5) were cocultured with freshly isolated autologous pDCs (10×10^4) in the presence of AEC-sups.

Statistics

Statistical analyses of all data were done with GraphPad Prism 5.0 software. Data were compared between groups using paired or unpaired Student *t* test and Spearman rank correlation.

RESULTS

VAT-Derived Chemerin Recruits pDCs in Obesity

We recruited adult obese individuals undergoing bariatric surgery and collected samples of their VAT. To explore the potential role of VAT-derived chemerin in recruitment of pDCs into VAT, we did explant cultures with human VAT samples. We found accumulation of chemerin in the AEC-sups with time (Fig. 1*A*). We then checked the chemotactic function of these AEC-sups in transwell migration

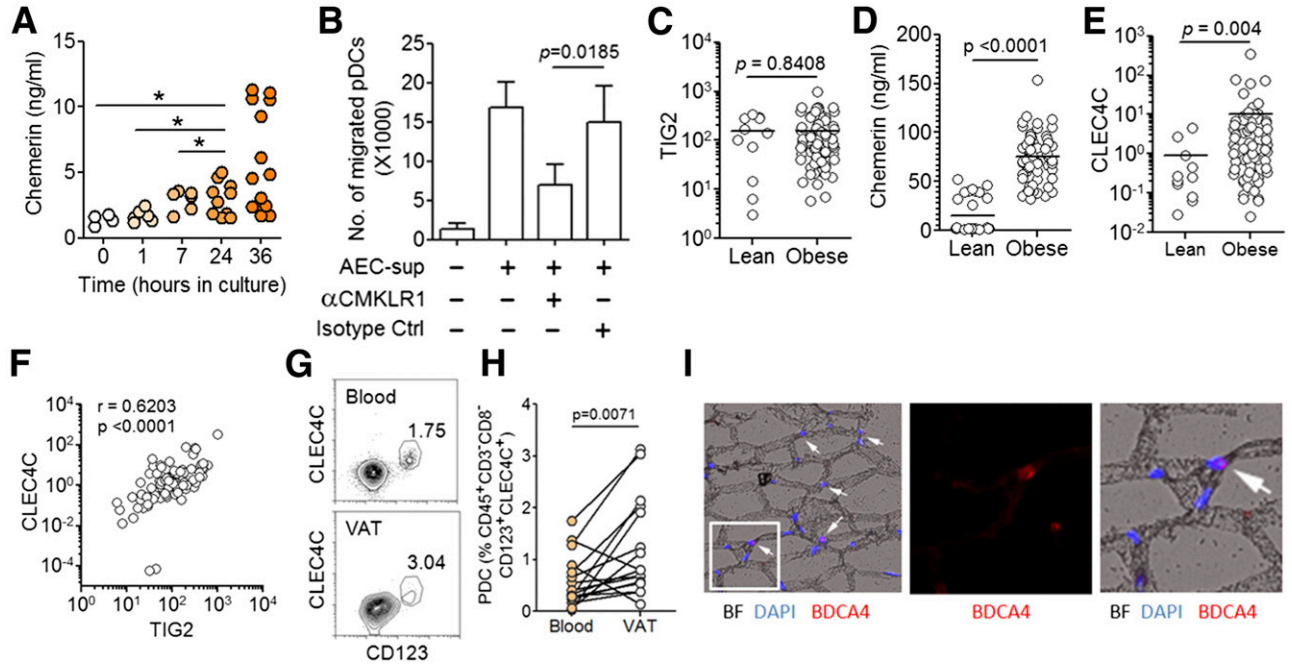

Figure 1—VAT-derived chemerin recruits pDCs in obesity. *A*: Chemerin ELISA was done on AEC-sups collected at various time points. Each dot represents an AEC-sup generated from different VAT samples ($n = 14$ at 36 h). Comparisons among paired samples were done by paired *t* test. *B*: Migration of pDC (isolated from healthy donors) was assessed in response to AEC-sups in transwells. pDCs were either untreated or pretreated with anti-CMKLR1 or isotype control antibody, and the number of migrated pDCs were compared by performing two-tailed paired *t* test ($P = 0.0185$). Cumulative data of six independent experiments (with different AEC-sup and pDC donor combinations) are represented. *C* and *E*: Total RNA was isolated from VAT of lean ($n = 11$) and obese ($n = 83$) individuals, and real-time PCR was done to determine the relative expression of CLEC4C and chemerin (TIG2) genes (normalized to the expression of 18S rRNA as the reference gene). Expression of TIG2 and CLEC4C was compared between the two groups by Student *t* test ($P = 0.8408$ for TIG2, $P = 0.004$ for CLEC4C). *D*: Plasma level of chemerin measured by ELISA was compared between lean and obese individuals by Student *t* test ($P < 0.0001$). *F*: The relative expression values of TIG2 and CLEC4C in obese VAT were correlated based on Spearman rank correlation ($r = 0.6203$, $P < 0.0001$). *G* and *H*: SVF was isolated from VAT samples by enzymatic digestion and stained to enumerate frequency of pDCs ($CD45^+CD3^-CD8^-CD123^+CLEC4c^+$ cells) by flow cytometry and compared with pDC frequency (stained similarly) from peripheral blood of the same individuals. A representative contour plot was acquired by flow cytometry (*G*), and a scatter plot reveals relative enrichment of pDCs in VAT (*H*) compared with peripheral blood ($n = 15$). Paired Student *t* test (two-tailed) was performed to show significant enrichment of pDCs in VAT ($P = 0.0071$). *I*: Representative images from immunofluorescence microscopy done on cryosections of VAT samples. The left panel shows the merged image of a 200× field; nuclei were stained with DAPI (blue), and pDCs were stained with PE-labeled anti-BDCA4 antibody (red). The middle panel shows a digitally zoomed region of the DAPI area, and the right panel shows the merged image of the same zoomed region of the field. Arrows show BDCA4$^+$ pDCs. *$P < 0.05$. BF, bright field; Ctrl, control.

experiments with purified pDCs from healthy donors. Neutralizing the receptor CMKLR1 led to total abolition of recombinant chemerin-induced pDC migration in these experiments (Supplementary Fig. 1*A*). We found efficient pDC migration along the AEC-sup gradient that also could be inhibited by neutralizing the CMKLR1 receptor on pDCs by using a monoclonal antibody as opposed to an isotype control antibody (Fig. 1*B*). Gene expression studies on these VAT samples revealed that VAT expression of TIG2 was not upregulated in obese compared with lean individuals (Fig. 1*C*), but plasma levels of chemerin were significantly higher in obese individuals (Fig. 1*D*). Thus, it seems that the increased volume of body visceral fat rather than the intrinsic biology of the adipose tissue is responsible for this increased plasma level of chemerin in obesity. Obese VAT also showed significantly higher enrichment of CLEC4C expression (Fig. 1*E*), the signature transcript for pDCs (20). We found a strong positive correlation between expression of chemerin (TIG2) and CLEC4C expression (Fig. 1*F*). Recruitment of other immune cell subsets in response to chemerin is implausible because expression of *CMKLR1*, the chemerin receptor, is restricted to pDCs among different immune cells (Supplementary Fig. 1*B*). We isolated the SVF from the collected VAT samples and detected significant enrichment of $CD45^+CD3^-CD8^-CD123^+CLEC4c^+$ pDCs by flow cytometry compared with peripheral blood (Fig. 1*G* and *H*). $BDCA4^+$ pDCs were also detected in situ in cryosections of VAT (Fig. 1*I*). These studies reveal that in obese individuals, adipose-derived chemerin can recruit pDCs from the circulation into the VAT through CMKLR1 receptor and thus link the hyperadiposity-driven functional phenotype of adipocytes to recruitment of a major innate immune cell.

Type I IFN Induction by VAT-Recruited pDCs

pDCs are the most efficient type I IFN–producing cells in the immune system (21). Induction of type I IFN production by pDCs in response to recognition of self or nonself nucleic acid molecules by endosomal TLRs (TLR9 and TLR7) is the mainstay of pDC function in protective immunity against pathogens (mostly viruses) as well as in their key role in several autoimmune diseases (18,19,21–23). Finding chemerin-driven recruitment of pDCs into VAT of obese individuals naturally led us to consider the possibility of pDC activation in situ and involvement of type I IFNs in metaflammation. We checked for expression of four genes (IRF7, ISG15, MX1, and TRIP14), which represent the group of IFN signature genes (ISGs) expressed in responder cells to type I IFN signaling that have previously been shown to be surrogate markers for type I IFN induction in several autoimmune contexts (24,25). We calculated an ISG index (ISGi) as the average relative expressions of the four selected ISGs (Supplementary Fig. 2*A*–*F*) and found that CLEC4C expression in VAT correlates positively with the ISGi (Fig. 2*A*). As expected, the ISGi was significantly higher in obese VAT than in lean VAT (Fig. 2*B*).

Previous studies have established that visceral fat depots are critical sites for obesity-associated metaflammation compared with subcutaneous adipose tissue (26). To confirm the importance of VAT in this phenomenon, we compared paired samples of subcutaneous adipose tissue with VAT samples (n = 6). As expected, VAT samples showed significantly higher expression of TIG2, enrichment of CLEC4C transcript, and ISGi (Supplementary Fig. 3*A*–*C*).

To look for endogenous molecules that may lead to type I IFN induction in VAT-recruited pDCs, we added AEC-sups collected from obese individuals to purified pDCs from healthy donors in culture. We found that AEC-sups could induce type I IFN production by pDCs (Fig. 2*C*). When AEC-sups were treated with DNase before addition to the culture, this pDC activation was abrogated, indicating that extracellular DNA molecules released in the AEC-sup play a role in pDC activation (Fig. 2*D*). Relative abundance of extracellular nucleic acids in VAT can be extrapolated from the higher propensity of adipocyte death and tissue remodeling previously reported in obesity (27,28). AEC-sups were also able to trigger TLR9 activation in HEK293 cells that express TLR9 and report downstream NF-κB activation through an enzymatic reporter (Fig. 2*E*). When the TLR9 gene was knocked down in pDCs using siRNAs (Supplementary Fig. 4*A*), AEC-sup–induced type I IFN production by pDCs was abolished (Fig. 2*F*), confirming a critical role of TLR9 activation in this event.

HMGB1 Aids Activation of VAT-Recruited pDCs

Under physiological conditions, extracellular nucleic acids of self-origin cannot access the TLRs in pDCs due to their endosomal localization (21). But in autoimmune contexts, endogenous molecules (e.g., LL37, HMGB1) take part in transport of self-nucleic acids into pDC endosomes and initiate sterile autoreactive inflammation (19,21). Among such molecules, the HMGB1 protein has been shown to bind extracellular self-DNA molecules and facilitate their recognition by endosomal TLR9 in pDCs through participation of RAGE, which is expressed in pDCs (29). Of note, one study showed that in obese individuals, there is an elevated level of HMGB1 in plasma as well as an increased expression in VAT, which correlate with adipose inflammatory markers (30). Therefore, we speculated that HMGB1 may help in TLR activation in VAT-recruited pDCs. Antibody-mediated neutralization of RAGE, the HMGB1 receptor, on pDCs could have inhibited AEC-sup–induced type I IFN induction (Fig. 3*A*). Moreover, antibody-mediated depletion of HMGB1 from the AEC-sups, before they were added to pDC cultures, abolished the type I IFN induction capability of the AEC-sup (Fig. 3*B*). Similar mechanisms of pDC activation seem to operate in vivo in obese individuals as well. We found a significantly positive correlation between expression of *HMGB1* and ISGi in VAT samples (Fig. 3*C*). Thus, we found that adipose tissue–derived HMGB1 and extracellular self-DNA molecules trigger TLR9 activation in pDCs aided

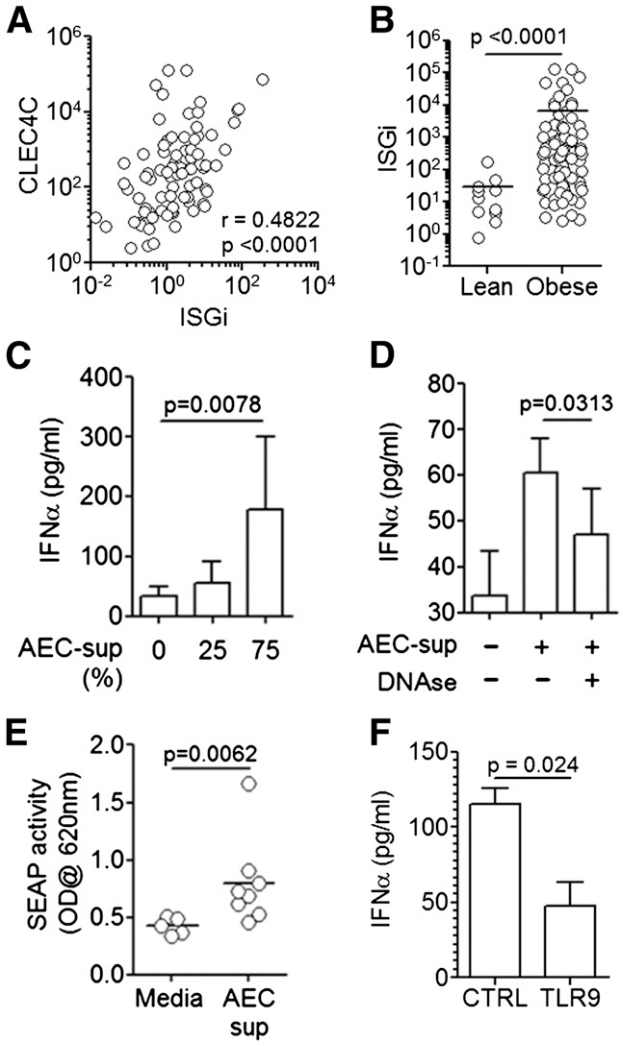

Figure 2—Type I IFN induction by VAT-recruited pDCs. *A*: Total RNA from VAT (n = 83) collected from obese individuals was isolated, and real-time PCR was done for the pDC-specific transcript CLEC4C and four ISGs, namely, IRF7, TRIP14, MX1, and ISG15; relative expression was quantified using 18S rRNA as the reference gene. ISGi was calculated as the average of the relative expressions of the four selected ISGs in each sample. The relative expression values of CLEC4C were then related with ISGi values based on Spearman rank correlation (r = 0.4822, $P < 0.0001$). *B*: Comparison of ISGi for VAT was compared between lean and obese individuals by Student t test ($P < 0.0001$). *C*: AEC-sup was added to pDCs from healthy donors in increasing doses (25% and 75% total volume of culture media), and after overnight incubation, supernatants were checked for presence of IFN-α by ELISA. Induction of IFN-α by AEC-sups was validated by paired t test (P = 0.0078). Cumulative data of seven independent experiments (with various AEC-sup and pDC donor combinations) are represented. *D*: AEC-sups were treated with DNase (as described in RESEARCH DESIGN AND METHODS) before addition to healthy pDC cultures. IFN-α induction (measured by ELISA on the supernatants after overnight incubation) was compared with AEC-sup without DNase treatment. Cumulative data of five independent experiments (with different AEC-sup and pDC donor combinations) are represented. *E*: AEC-sup (25% of total volume of 200 μL per well) were added to HEK293 cells expressing TLR9 and reported downstream NF-κB activation through SEAP reporter. Supernatants were collected after 12 h and added to an SEAP substrate medium for further incubation. Optical density (OD) was then measured at 620 nm on a spectrophotometer. Data from eight different AEC-sups are presented and compared with control medium–induced enzyme activity by unpaired t test (P = 0.0062). *F*: TLR9 gene expression was knocked down in pDCs isolated from healthy individuals by using RNA interference. Knockdown efficiency is presented in Supplementary Fig. 4*A*. Control (for EGFP) and target (for TLR9) siRNA-transfected cells were cultured in the presence of AEC-sup (75% of total volume of 100 μL per well), and after overnight incubation, IFN-α was measured in culture supernatants. Data from seven independent experiments are presented. Comparison between control and target-transfected cells were done by two-tailed paired t test (P = 0.024). CTRL, control.

by RAGE receptors on pDCs, leading to induction of type I IFN production in situ.

Type I IFNs Polarize Macrophages to a Proinflammatory Phenotype

A mechanistic link between accumulation and proinflammatory polarization of macrophages in VAT is established in obesity-associated metaflammation (3,4,31). Macrophages in lean adipose tissue show an alternatively activated anti-inflammatory M2 phenotype, whereas in obese adipose tissue, they show a classically activated proinflammatory M1 phenotype (3,31). Whether this results from selective recruitment of M1-like macrophages into VAT or is due to in situ polarization of M2 to the M1 phenotype remains an open question. We wanted to explore whether type I IFN induction in VAT can drive in situ polarization of M2 macrophages to the proinflammatory M1 phenotype. First, to check whether this can happen in vitro, we generated M2 macrophages from $CD14^+$ monocytes isolated from peripheral blood of healthy individuals in the presence of M-CSF and IL-4. We found that these in vitro–generated M2 macrophages could be polarized to a proinflammatory M1-like phenotype in the presence of recombinant IFN-α in terms of reduction in expression of M2-specific genes, like F13A1 and CCL22 (Fig. 4*A* and *B*), and surface expression of the mannose receptor CD206, an established marker for M2 macrophages generated in vitro in response to IL-4 (32) (Fig. 4*E* and *F*). Expression of IFN regulatory factor 5 (IRF5), a transcription factor with an established role in proinflammatory polarization of macrophages (33,34), and the gene for inducible nitric oxide synthase (NOS2), which is characteristically expressed in M1 macrophages, were increased in the presence of IFN-α (Fig. 4*C* and *D*). Surface expression of the costimulatory molecule CD86, characteristic of M1-like proinflammatory macrophages (35), was also enhanced in the presence of IFN-α (Fig. 4*E* and *F*). Constitutive TNF-α production was also enhanced in the macrophage cultures in the presence of IFN-α (Fig. 4*G*). Thus, we found that IFN-α, the major member of type I IFN family, can drive polarization of alternatively activated macrophages to a proinflammatory phenotype in vitro.

Role of Type I IFNs in Macrophage Polarization In Situ

To confirm the role of pDCs in polarization of M2 to M1 macrophages in response to VAT-derived TLR9 ligands,

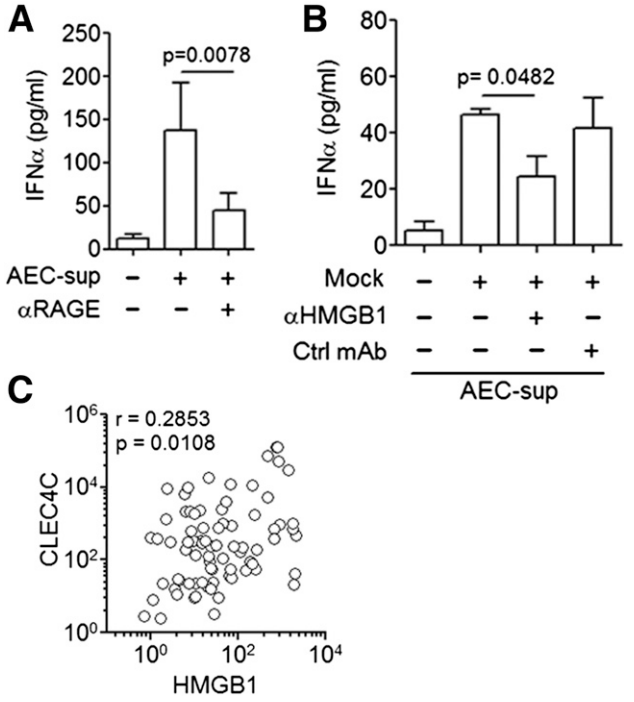

Figure 3—HMGB1 aids activation of VAT-recruited pDCs. *A*: AEC-sups (75% of total volume 100 μL per well) were added to healthy pDC cultures and incubated overnight. In some conditions before addition of AEC-sups, pDCs were treated with an anti-RAGE goat polyclonal antibody. ELISA was done to compare IFN-α levels in supernatants of anti-RAGE antibody–treated or untreated pDCs. Cumulative data of seven independent experiments (with different AEC-sup and pDC donor combinations) are represented. Comparison between antibody-treated and untreated conditions was done by one-tailed paired *t* test ($P = 0.0078$). *B*: HMGB1 was depleted from AEC-sups by using a monoclonal antibody (mAb) and protein G magnetic beads. These AEC-sups were then added (75% of total volume 100 μL per well) to pDC cultures and incubated overnight. ELISA was done for IFN-α on the supernatants and compared between HMGB1-depleted or control antibody–depleted AEC-sup treatments by unpaired *t* test ($P = 0.0482$). *C*: Total RNA from VAT ($n = 79$) was isolated, and real-time PCR was done for HMGB1, and the relative expression of the four ISGs (IRF7, TRIP14, MX1, and ISG15) was quantified using 18S rRNA as the reference gene. The relative expression values of CLEC4C were then related with ISGi values based on Spearman rank correlation ($r = 0.2853$, $P = 0.0108$). Ctrl, control.

we performed coculture experiments of in vitro–generated M2 macrophages and freshly isolated pDCs in the presence of AEC-sup (Fig. 5*A*). We found that the proinflammatory polarization of the M2 macrophages in response to AEC-sup was significantly reduced in the absence of cocultured pDCs in terms of surface expression of M2-specific marker CD206 (Fig. 5*B*) and M1-specific marker CD86 (Fig. 5*C*). This was associated with a significant reduction in accumulation of IFN-α in the supernatant (Fig. 5*D*).

To further validate the putative role of type I IFN response in in situ M1 polarization of the VAT-resident macrophages, we isolated M1- and M2-type resident macrophages from the SVFs of VAT from obese individuals by flow cytometric sorting. Expression of surface markers CD206 and CD86, used for assessing in vitro generation of M1 and M2 phenotypes, did not distinguish these phenotypic subsets in SVF, which is not surprising because characteristic markers of macrophage subsets vary between contexts (36). Adipose tissue resident M2 macrophages can be identified by expression of CD163, whereas M1 macrophages present in obese VATs express CD11c (35,37,38). Accordingly, we could define distinct subsets of M1 and M2 macrophages in SVF isolated from VAT samples as $CD45^+CD11b^+CD11c^+$ and $CD45^+CD11b^+CD163^+$ cells, respectively (Fig. 5*E*). Apart from the surface markers, the subsets could also be validated based on expression IRF5 (Fig. 5*F*) and NOS2 (Fig. 5*G*). We found that expression of the ISG genes was significantly enriched in the $CD11c^+$ M1 subset (Fig. 5*H*), indicating that a type I IFN response in the adipose resident macrophages favors M1 polarization. The expression of IRF5 and NOS2 in the $CD11c^+$ M1 macrophages strongly correlated with ISGi values as well (Fig. 5*I* and *J*).

In a few studies done in murine models of HFD-induced metabolic syndrome, TLR9 activation in macrophages in response to circulating DNA has been implicated in proinflammatory polarization of macrophages (39,40). In humans, however, TLR9 expression is restricted to pDCs and B cells, with no considerable expression in the myeloid compartments, as opposed to that in mice (41). To confirm this, we also compared expression of TLR9 in circulating pDCs, B cells, T cells, conventional DCs, monocytes, and in vitro–generated and ex vivo–isolated M1 and M2 macrophages. We found pDCs to be the major TLR9-expressing cells, with no significant expression in any of the myeloid cell subset as previously described (Supplementary Fig. 4*B*). In whole-tissue transcripts from VAT as well, expression of genes characteristic of M1 macrophages (namely, IRF5) was found to be significantly correlated with the level of type I IFN induction (in terms of ISGi values) in VAT (Fig. 6*A*) and with expression of the pDC signature gene CLEC4C (Fig. 6*B*). Although a significantly coherent expression of IRF5 and NOS2 in VAT validated their selection as M1 signature genes (Supplementary Fig. 5*A*), in total VAT transcript analysis, NOS2 expression was not correlated with ISGi perhaps because of a type I IFN–independent regulation of its expression in cells other than macrophages in vivo (Supplementary Fig. 5*B*). The ratio of frequency of M1 and M2 macrophages in the SVF from VATs ($n = 11$) was also found to be correlated with VAT ISGi (Fig. 6*C*). Thus, we found that induction of type I IFNs in VAT of obese individuals drives in situ proinflammatory polarization of macrophages as characterized by key signature genes and surface markers, thereby fueling metaflammation.

Type I IFN Induction in VAT Is Associated With IR

Because proinflammatory polarization of VAT-recruited macrophages has been linked to systemic IR in numerous previous studies (3,31), we expected a link between level of type I IFN induction in obese VAT with adipose tissue

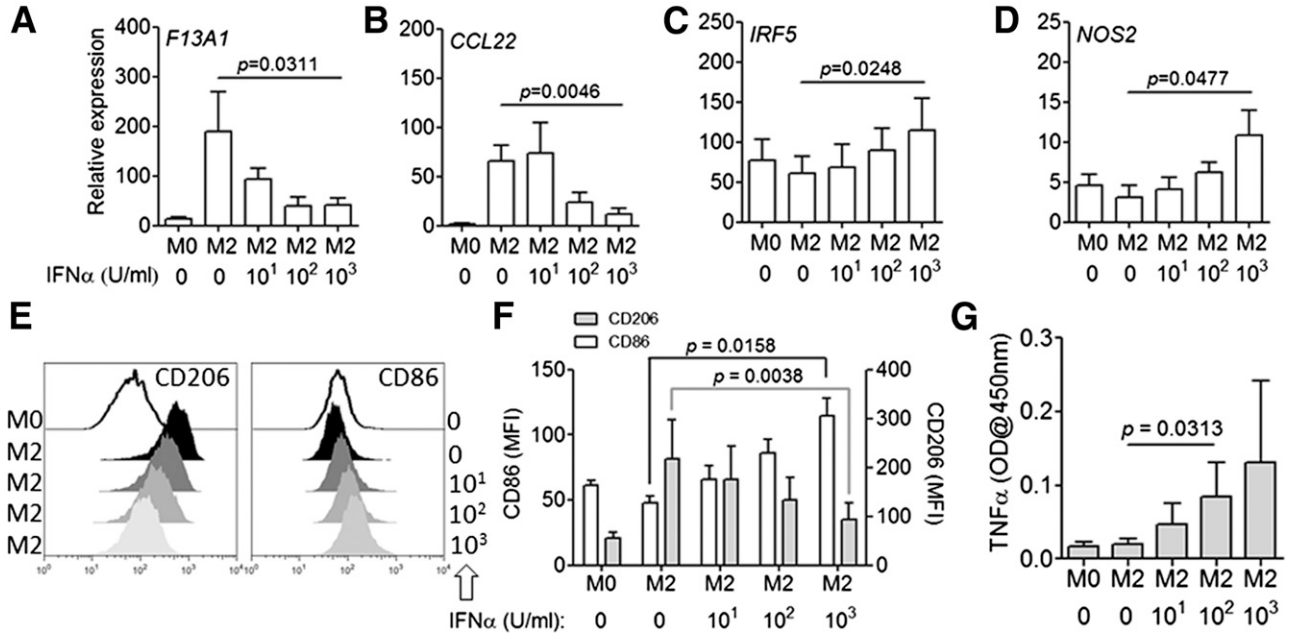

Figure 4—Proinflammatory macrophage polarization by type I IFNs. *A–D*: CD14$^+$ monocytes isolated from peripheral blood of healthy donors were developed into macrophages in vitro in the presence of M-CSF and then into M2-type macrophages by adding recombinant human IL-4 in the culture. The cells were further cultured in the absence or presence of escalating doses of recombinant human IFN-α. Total RNA was then isolated from the cells, and real-time PCR was done for two M2 signature genes, *F13A1* (*A*) and *CCL22* (*B*), as well as for two M1 signature genes, *IRF5* (*C*) and *NOS2* (*D*). In the presence of IFN-α, the M2-polarized cells showed a reduction in the M2 signature genes and induction of the M1 signature genes. Statistical significance was checked by paired *t* test. Cumulative data of three to seven independent experiments are presented. *E* and *F*: Macrophages generated as described in *A–D* were assessed for surface expression of the M2-specific marker CD206 and the M1-specific marker CD86 by flow cytometry. Histograms of a representative experiment for both the markers (*E*) and cumulative data of mean fluorescence intensity (MFI) from five independent experiments (*F*) are shown. Statistical significance was checked by two-tailed paired *t* test. *G*: ELISA was done for TNF-α on supernatants collected at the end of the culture from the macrophages generated as described previously; absorbance was taken at 450 nm (P = 0.0313 by Wilcoxon matched pair signed rank test). OD, optical density.

and systemic IR. We assessed adipose tissue IR in the recruited obese individuals by measuring the ADIPO-IR index (ADIPO-IR = plasma FFAs × insulin concentration), which has been validated previously for this purpose (42). Of note, we identified two distinct groups of individuals in whom VAT ISGi was positively correlated with ADIPO-IR values (Fig. 7*A–C*). One group (left-shifted correlation [group L]), however, had higher ADIPO-IR values corresponding to its ISGi values than the other group (right-shifted correlation [group R]). We also found a significant positive correlation of HOMA2-IR values, which indicate systemic IR, with VAT ISGi in both groups L and R (Fig. 7*D* and *E*). These groups were not significantly different with respect to BMI (Supplementary Fig. 6*A*), but group R showed significantly higher enrichment of the pDC-specific transcript CLEC4C, higher ISGi, and higher expression of the M1 macrophage signature IRF5 (Supplementary Fig. 6*B–D*). These two distinct groups perhaps point to different susceptibility of obese individuals to the development of IR after the innate initiation of metaflammation through type I IFNs. Of note, the level of glycated hemoglobin (HbA_{1c}) was significantly correlated with only group R (Fig. 7*F*), indicating that higher levels of ISGi have a greater influence on long-term glycemic control. Thus, we have unraveled a hitherto unknown pathway for the initiation of metaflammation that links obesity-induced functional changes in VAT with recruitment and activation of a major innate immune mechanism, which can both initiate and fuel metaflammation as shown in the pathogenetic model (Fig. 7*G*).

DISCUSSION

Despite recent advances in the understanding of adipose tissue inflammation and its role in IR, all key contributions from the immune cell subsets are yet to be fully understood. Although the fetuin-A-TLR4 axis in adipocytes and resulting MCP1 expression in visceral fat depots has been implicated in the recruitment of circulating CCR2$^+$ monocytes into VAT, the mechanism of their polarization into proinflammatory macrophages is not clear, as discussed earlier. We found that chemerin, an adipokine shown to be produced by adipocytes in response to FFAs with reported abundance in plasma in obese individuals, plays a role in the innate initiation of VAT inflammation. Chemerin is known to have chemoattractant properties in cells expressing its cognate receptor CMKLR1, which is preferentially expressed on the pDCs among immune cells. We believe that as the VAT depots become

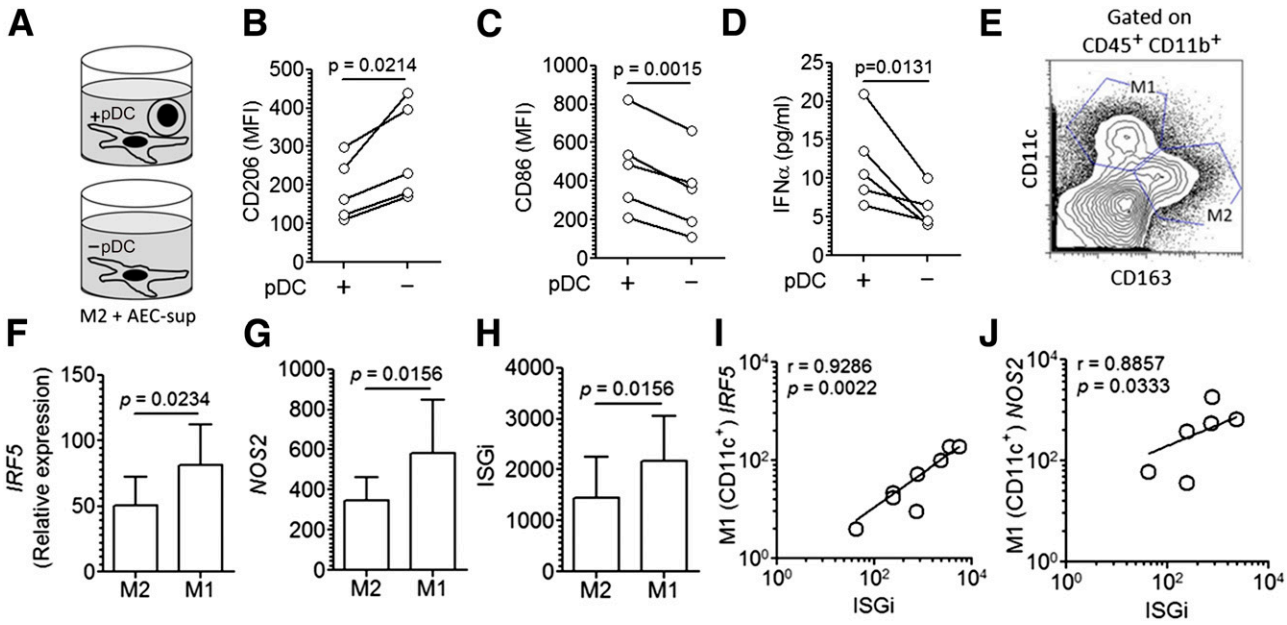

Figure 5—Role of pDCs and type I IFNs in proinflammatory polarization of macrophages in the context of metaflammation. *A–C*: In vitro–generated M2 macrophages were cultured with AEC-sup (75% of total volume 200 μL per well) in the presence or absence of autologous pDCs (*A*). After 2 days, cells were harvested and used for flow cytometric assessment of M2-specific surface marker CD206 (*B*) and M1-specific surface marker CD86 (*C*) on $CD11b^+$ macrophages. *D*: Culture supernatants from the coculture experiment described in *A* were harvested, and IFN-α was measured by ELISA; the comparison was done by paired *t* test ($P = 0.0131$). *E*: SVF was isolated from VAT samples by enzymatic digestion and stained to isolate M1-type ($CD45^+CD11b^+CD11c^+$ cells) and M2-type ($CD45^+CD11b^+CD163^+$ cells) by flow cytometry; a representative contour plot is shown. *F* and *G*: Total RNA was isolated from the sorted M1-type and M2-type cells, and expression data from quantitative PCR for two M1 signature genes, *IRF5* (*F*) and *NOS2* (*G*), were compared between two subsets ($n = 7$). *H*: ISGi (calculated as the average of expression of four ISGs [IRF7, TRIP14, MX1, and ISG15]) was compared between M2 and M1 macrophages ($n = 7$). *I* and *J*: Relative expression of ISGs (ISGi) was correlated with relative expression of IRF5 and NOS2 in the sorted $CD11c^+$ M1 macrophages based on Spearman rank correlation (IRF5 vs. ISGi: $n = 7$, $r = 0.9286$, $P = 0.0022$; NOS2 vs. ISGi: $n = 6$, $r = 0.8857$, $P = 0.0333$). MFI, mean fluorescence intensity.

a source of chemerin in obesity, circulating pDCs infiltrate VAT in response to CMKLR1 triggering, thus linking hyperadiposity to VAT recruitment of an innate immune cell. Although obese individuals had significantly higher levels of chemerin in plasma than lean individuals, VAT expression of chemerin (TIG2) showed no difference between the groups, indicating a dependence of systemic abundance of chemerin on total volume of VAT rather than change in adipose biology in obesity. Total VAT volume has also been shown previously to be linked with extent of inflammation (26). As expected, both enrichment of pDC transcript CLEC4C expression in VAT and ISGi were significantly higher in obese than in lean individuals. Of note, we did not find a correlation between BMI with plasma chemerin levels in obese individuals, which may be a result of ongoing therapy with antidiabetic drugs, especially metformin, in a large number of these individuals. The reduction in level of chemerin in response to drug therapy has been previously established (43).

$CD11c^+$ DC recruitment into VAT has been previously reported, but these studies focused mainly on conventional DCs (cDCs) and their role in T-cell polarization. DC infiltration into the VAT and liver has also been correlated with macrophage infiltration in HFD-fed mice genetically deficient in $CD11c^+$ DCs (44). Although in this study VAT-infiltrating DCs comprised both cDCs and pDCs, the phenotype was linked to the role of cDCs (44). Another study provided evidence for $CD11c^+$ cell recruitment in VAT of obese individuals and showed that ablation of $CD11c^+$ DCs in HFD-fed obese mice reduced VAT inflammation as well as IR (45). The reason behind this recruitment of DCs and initiation of the metaflammation process, however, was not clear in these studies.

pDCs are the major producers of type I IFNs in the body (21), and the role of pDC-derived type I IFNs in initiating autoreactive inflammation in several autoimmune disease is well established (18,19,22,23). In the current study, we show the possible mechanism of activation of VAT-recruited pDCs by free self-DNA molecules released from adipose tissue. pDC activation and consequent type I IFN induction depended on HMGB1 bound to the DNA molecules and RAGE receptor on pDCs. Other findings of amelioration of disease in HFD-fed mice with genetic deficiency of RAGE (46) as well as of increased concentration of circulating HMGB1 in obese individuals with metabolic syndrome (30) support this possibility. An increased adipose tissue turnover and adipocyte death in obese individuals can be responsible for the abundance of both HMGB1 and the free nucleic acid molecules.

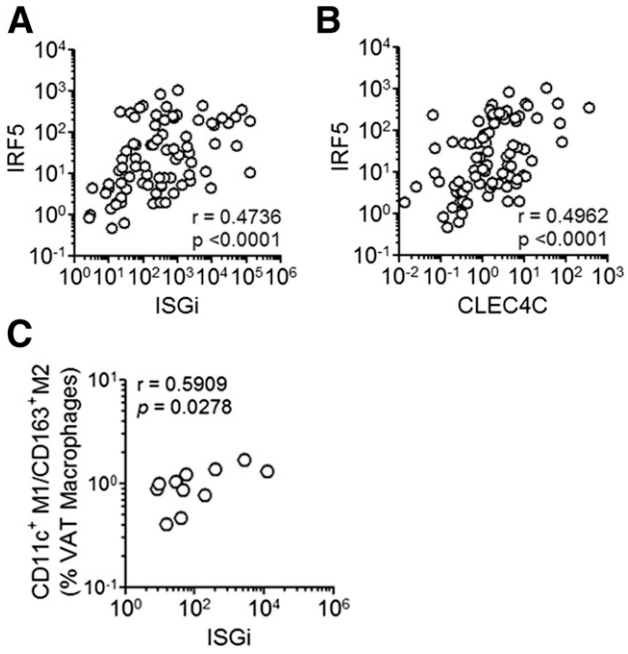

Figure 6—Relating tissue type I IFN response to macrophage composition. *A* and *B*: Correlation of VAT expression of IRF5 with tissue ISGi (n = 82, Spearman r = 0.4736, $P < 0.0001$) and VAT expression of the signature pDC transcript CLEC4C (n = 82, Spearman r = 0.4962, $P < 0.0001$). *C*: Ratio of M1 ($CD11c^+$) to M2 ($CD163^+$) macrophage frequency (% of $CD45^+CD11b^+$ cells) in VAT was related with whole-tissue ISGi based on Spearman rank correlation (n = 11, r = 0.5909, P = 0.0278).

TLR9 recognizes unmethylated CpG motifs on DNA molecules (21). Both genomic and mitochondrial DNA contain such motifs, and their release in response to adipocyte death can trigger TLR9 activation in pDCs when aided by molecules like HMGB1. Recently, plasma from both HFD-fed mice and patients with nonalcoholic steatohepatitis was shown to have circulating mitochondrial DNA, which contributes to hepatic inflammation and disease through TLR9 triggering (39). A recent study showed that TLR9 activation in VAT-recruited macrophages in response to cell free DNA from dying adipocytes induced CCL2 expression in situ (40). Accordingly, in $TLR9^{-/-}$ HFD-fed mice, accumulation of macrophages in VAT, VAT-resident inflammation, and IR were attenuated. Of note, in both these murine studies, the whole phenotype was shown to depend on TLR9 expression in lysozyme-expressing macrophages, whereas in humans, TLR9 expression is largely restricted in pDCs and B cells (41). The second study also found that the level of circulating DNA molecules, the TLR9 ligands, was increased in obese individuals and correlated with their systemic IR (40).

In clinical contexts of autoimmune disorders, pDC-derived type I IFNs drive inflammation by influencing cDC maturation as well as potentiation of autoreactive B-cell activation and expansion (47,48). We now have unraveled a direct action of type I IFNs on the VAT-recruited macrophages. We provide evidence of polarization of M2 macrophages to the proinflammatory M1 phenotype in response to type I IFNs both in vitro and in situ. The phenotypic details of in vitro–generated and ex vivo–isolated macrophages were somewhat different in terms of gene expression and surface markers, probably due to additional microenvironmental factors in vivo. Among the ex vivo–isolated macrophages, we could identify and isolate $CD163^+$ M2 and $CD11c^+$ M1 subsets as described (2). The ex vivo–isolated M1 macrophages had a clear enrichment of ISG expression. In a previous study, again in the HFD-fed mouse model, $CD11c^+$ macrophages were shown to be instrumental for adipose inflammation and IR (49), as shown by disease amelioration on genetic deficiency of $CD11c^+$ cells. But in that study, the phenotype might have contributions from both infiltrating DCs (pDCs and cDCs) and M1 macrophages because all of them express CD11c.

VAT infiltration of a number of other immune cells has been implicated in metaflammation other than macrophages and DCs (3,50). The cellular components of the adaptive immune system, namely T-helper 1–polarized CD4 cells (51) and cytotoxic CD8 T cells (52), perhaps get involved downstream of innate initiation of metaflammation. But recently, in situ activation of VAT-resident natural killer (NK) cells, an innate immune cell subset, was found to be a critical driver of metaflammation in independent studies using two different genetic models of NK-cell deficiency as well as in obese humans (53,54). Of note, a critical role of type I IFNs was established in the regulation of NK-cell function in such contexts as viral infection and solid tumors (55–57). A recent study also established that NK-cell activation and survival is severely impaired in the absence of type I IFNs (58). Thus, plausibly, in situ induction of type I IFNs in VAT, as reported by us, mechanistically precedes activation of NK cells during metaflammation.

We found that induction of type I IFN in VAT was linked to both adipose tissue (represented by ADIPO-IR) and systemic IR (represented by HOMA2-IR), although it was not correlated individually with fasting blood glucose, FFA, or insulin levels in plasma (data not shown). We could identify, however, two subgroups among obese individuals with different susceptibility of insulin unresponsiveness in the adipose tissue to the level of type I IFN induction in situ. Group L had higher ADIPO-IR levels at lower VAT ISGi compared with group R. HOMA2-IR was similarly regulated in response to VAT ISGi. Of note, the level of HbA_{1c} was correlated with VAT ISGi only in group R, perhaps pointing to higher ISGi levels affecting long-term glycemic control to a greater extent.

A putative role of type I IFNs in systemic IR was suggested a long time ago in a study wherein IR developed in human subjects injected with IFN-α (59). Pegylated IFN-α therapy in patients with hepatitis C viral infection was also found to be associated with IR (60,61). Genetic deficiency of IRF7 (IFN regulatory factor 7), the critical transcription factor for induction of type I IFNs in

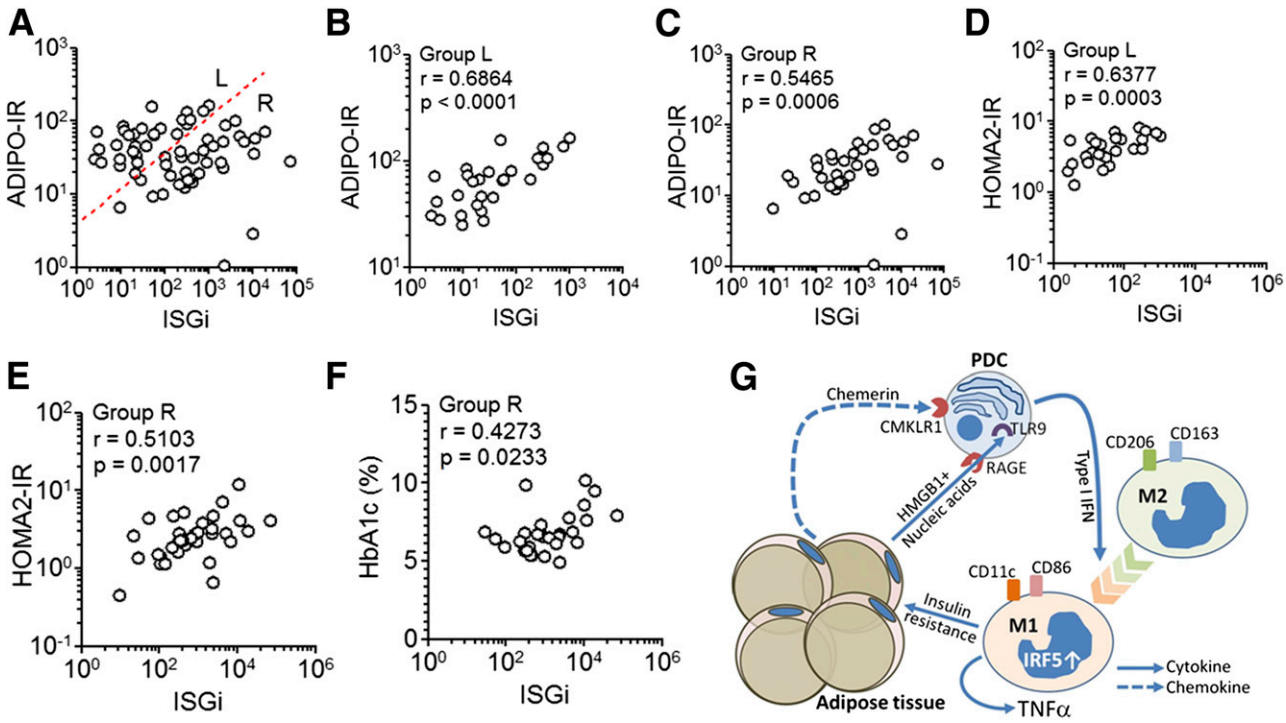

Figure 7—Relationship between VAT type I IFN induction with IR and the proposed model for the role of pDCs in metaflammation. *A–C*: IR in adipose tissue was assessed using the ADIPO-IR index and calculated from circulating FFA and insulin levels, and the relationship between VAT ISGi and corresponding ADIPO-IR values are shown. Two distinct groups, one with a left-shifted correlation (group L) and another with a right-shifted correlation (group R) are demarcated by the dashed line (*A*). The same correlation in the individual groups are shown in *B* and *C*. *D* and *E*: HOMA2-IR was calculated using levels of fasting blood glucose and insulin. The relationship between VAT ISGi and corresponding HOMA2-IR values are shown for group L (Spearman $r = 0.6377$, $P = 0.0003$) and group R (Spearman $r = 0.5103$, $P = 0.0017$). *F*: Relationship between VAT ISGi and corresponding HbA_{1c} values are shown for group R (Spearman $r = 0.4273$, $P = 0.0233$). *G*: The model based on the data proposes that VAT-derived chemerin recruits circulating pDCs through the CMKLR1 receptor. VAT-recruited pDCs are activated in situ by HMGB1-nucleic acid complexes that may access TLR9 in pDCs through RAGE receptors. pDCs thus activated produce type I IFNs in situ, which in turn can fuel in situ polarization of M2 macrophages to proinflammatory M1 macrophages expressing IRF5. The proinflammatory M1 macrophages in turn contribute to propagation of chronic inflammation in VAT and to IR.

pDCs (62), was found to protect mice from HFD-induced metabolic syndrome (63). In clinical contexts, an associated risk of developing metabolic disorders has already been established in systemic lupus erythematosus (64) and psoriasis (65), where pDC-derived type I IFNs play a central role in pathogenesis (19). Administration of hydroxychloroquine (HCQ), the antimalarial drug with antirheumatic effects, was found to improve insulin sensitivity in obese individuals (66,67). The role of HCQ in inhibition of endosomal TLRs, either by regulation of endosomal acidification or direct interaction with the nucleic acid ligands, is established (68,69). We speculate that the antidiabetic effect of HCQ is also through inhibition of TLR-mediated type I IFN induction. Of note, the level of systemic IR in the current study represents both the influence of metaflammation and the intrinsic insulin unresponsiveness in metabolically active tissues. Thus, beyond contribution to metaflammation, the role of type I IFNs in driving systemic IR by direct action on metabolically active tissues needs to be explored. In fact, hepatic IR in response to IFN-α was suggested in a previous study (70).

In conclusion, we propose a novel model (Fig. 7*G*) for the initiation of metaflammation in obese individuals wherein adipose recruitment of pDCs in response to high expression of chemerin and in situ TLR activation in adipose-recruited pDCs in response to HMGB1-nucleic acid complexes lead to induction of type I IFNs. Type I IFNs in turn fuel metaflammation by driving proinflammatory polarization of macrophages in VAT and contribute to systemic IR. Type I IFNs are already being explored as therapeutic targets in various systemic autoimmune contexts (71,72). This study also opens the possibility of similar therapeutic approaches in obesity-associated metabolic syndrome.

Acknowledgments. The authors thank Utpalendu Ghosh and Suvendra Nath Bhattacharyya (Council of Scientific and Industrial Research [CSIR]-Indian Institute of Chemical Biology) for help with cryosections and nucleofection experiments, respectively.

Funding. A.R.G. and O.R. are supported by senior research fellowships from the University Grants Commission, India. R.B. and T.N. received CSIR senior research fellowships. D.R. and C.S.C.L. are supported by CSIR junior research fellowships. S.Bh. is supported by a research associateship from the Government of India's Department of Biotechnology. The study was supported by the

Government of India's Science and Engineering Board's Ramanujan Fellowship and CSIR network project grants BSC0206 (to P.C.) and BSC0114 (to D.G.).

Duality of Interest. No potential conflicts of interest relevant to this article were reported.

Author Contributions. A.R.G. did the patient sampling, performed most of the experiments, and analyzed data. R.B. contributed the pDC activation studies, gene expression studies, patient sampling, and data collection. S.Bh. and D.R. contributed to the gene expression studies. T.N. contributed to the SVF studies, patient sampling, and data collection. O.R. contributed to the gene expression studies. P.D. and C.S.C.L. contributed to the patient sampling and data collection. S.R. contributed to the pDC activation studies. P.G. and S.M. contributed to the clinical evaluation and stratification of recruited patients. S.K., T.C., and O.T. contributed to the recruitment of patients and bariatric surgical procedures. S.H. and P.C. contributed the clinical evaluation and stratification of recruited patients and data analysis. S.Ba. contributed to the flow cytometry. D.G. contributed to the study concept and design, data analysis, and writing of the manuscript. D.G. is the guarantor of this work and, as such, had full access to all the data in the study and takes responsibility for the integrity of the data and the accuracy of the data analysis.

References

1. Gregor MF, Hotamisligil GS. Inflammatory mechanisms in obesity. Annu Rev Immunol 2011;29:415–445
2. Chawla A, Nguyen KD, Goh YP. Macrophage-mediated inflammation in metabolic disease. Nat Rev Immunol 2011;11:738–749
3. Mathis D. Immunological goings-on in visceral adipose tissue. Cell Metab 2013;17:851–859
4. Weisberg SP, McCann D, Desai M, Rosenbaum M, Leibel RL, Ferrante AW Jr. Obesity is associated with macrophage accumulation in adipose tissue. J Clin Invest 2003;112:1796–1808
5. Weisberg SP, Hunter D, Huber R, et al. CCR2 modulates inflammatory and metabolic effects of high-fat feeding. J Clin Invest 2006;116:115–124
6. Oh DY, Morinaga H, Talukdar S, Bae EJ, Olefsky JM. Increased macrophage migration into adipose tissue in obese mice. Diabetes 2012;61:346–354
7. Sierra-Filardi E, Nieto C, Domínguez-Soto A, et al. CCL2 shapes macrophage polarization by GM-CSF and M-CSF: identification of CCL2/CCR2-dependent gene expression profile. J Immunol 2014;192:3858–3867
8. Shi H, Kokoeva MV, Inouye K, Tzameli I, Yin H, Flier JS. TLR4 links innate immunity and fatty acid-induced insulin resistance. J Clin Invest 2006;116:3015–3025
9. Kim JK. Fat uses a TOLL-road to connect inflammation and diabetes. Cell Metab 2006;4:417–419
10. Pal D, Dasgupta S, Kundu R, et al. Fetuin-A acts as an endogenous ligand of TLR4 to promote lipid-induced insulin resistance. Nat Med 2012;18:1279–1285
11. Ouchi N, Parker JL, Lugus JJ, Walsh K. Adipokines in inflammation and metabolic disease. Nat Rev Immunol 2011;11:85–97
12. Ernst MC, Sinal CJ. Chemerin: at the crossroads of inflammation and obesity. Trends Endocrinol Metab 2010;21:660–667
13. Bauer S, Wanninger J, Schmidhofer S, et al. Sterol regulatory element-binding protein 2 (SREBP2) activation after excess triglyceride storage induces chemerin in hypertrophic adipocytes. Endocrinology 2011;152:26–35
14. Ernst MC, Haidl ID, Zúñiga LA, et al. Disruption of the chemokine-like receptor-1 (CMKLR1) gene is associated with reduced adiposity and glucose intolerance. Endocrinology 2012;153:672–682
15. Li Y, Shi B, Li S. Association between serum chemerin concentrations and clinical indices in obesity or metabolic syndrome: a meta-analysis. PLoS One 2014;9:e113915
16. Zabel BA, Silverio AM, Butcher EC. Chemokine-like receptor 1 expression and chemerin-directed chemotaxis distinguish plasmacytoid from myeloid dendritic cells in human blood. J Immunol 2005;174:244–251
17. Vermi W, Riboldi E, Wittamer V, et al. Role of ChemR23 in directing the migration of myeloid and plasmacytoid dendritic cells to lymphoid organs and inflamed skin. J Exp Med 2005;201:509–515
18. Ganguly D, Chamilos G, Lande R, et al. Self-RNA-antimicrobial peptide complexes activate human dendritic cells through TLR7 and TLR8. J Exp Med 2009;206:1983–1994
19. Ganguly D, Haak S, Sisirak V, Reizis B. The role of dendritic cells in autoimmunity. Nat Rev Immunol 2013;13:566–577
20. Dzionek A, Sohma Y, Nagafune J, et al. BDCA-2, a novel plasmacytoid dendritic cell-specific type II C-type lectin, mediates antigen capture and is a potent inhibitor of interferon alpha/beta induction. J Exp Med 2001;194:1823–1834
21. Gilliet M, Cao W, Liu YJ. Plasmacytoid dendritic cells: sensing nucleic acids in viral infection and autoimmune diseases. Nat Rev Immunol 2008;8:594–606
22. Lande R, Gregorio J, Facchinetti V, et al. Plasmacytoid dendritic cells sense self-DNA coupled with antimicrobial peptide. Nature 2007;449:564–569
23. Sisirak V, Ganguly D, Lewis KL, et al. Genetic evidence for the role of plasmacytoid dendritic cells in systemic lupus erythematosus. J Exp Med 2014;211:1969–1976
24. Bennett L, Palucka AK, Arce E, et al. Interferon and granulopoiesis signatures in systemic lupus erythematosus blood. J Exp Med 2003;197:711–723
25. Rönnblom L, Eloranta ML. The interferon signature in autoimmune diseases. Curr Opin Rheumatol 2103;25:248–253
26. Sam S, Haffner S, Davidson MH, et al. Relation of abdominal fat depots to systemic markers of inflammation in type 2 diabetes. Diabetes Care 2009;32:932–937
27. Cinti S, Mitchell G, Barbatelli G, et al. Adipocyte death defines macrophage localization and function in adipose tissue of obese mice and humans. J Lipid Res 2005;46:2347–2355
28. Strissel KJ, Stancheva Z, Miyoshi H, et al. Adipocyte death, adipose tissue remodeling, and obesity complications. Diabetes 2007;56:2910–2918
29. Tian J, Avalos AM, Mao SY, et al. Toll-like receptor 9-dependent activation by DNA-containing immune complexes is mediated by HMGB1 and RAGE. Nat Immunol 2007;8:487–496
30. Guzmán-Ruiz R, Ortega F, Rodríguez A, et al. Alarmin high-mobility group B1 (HMGB1) is regulated in human adipocytes in insulin resistance and influences insulin secretion in β-cells. Int J Obes 2014;38:1545–1554
31. Odegaard JI, Chawla A. Pleiotropic actions of insulin resistance and inflammation in metabolic homeostasis. Science 2013;339:172–177
32. Stein M, Keshav S, Harris N, Gordon S. Interleukin 4 potently enhances murine macrophage mannose receptor activity: a marker of alternative immunologic macrophage activation. J Exp Med 1992;176:287–292
33. Krausgruber T, Blazek K, Smallie T, et al. IRF5 promotes inflammatory macrophage polarization and TH1-TH17 responses. Nat Immunol 2011;12:231–238
34. Dalmas E, Toubal A, Alzaid F, et al. Irf5 deficiency in macrophages promotes beneficial adipose tissue expansion and insulin sensitivity during obesity. Nat Med 2015;21:610–618
35. Shaul ME, Bennett G, Strissel KJ, Greenberg AS, Obin MS. Dynamic, M2-like remodeling phenotypes of CD11c+ adipose tissue macrophages during high-fat diet–induced obesity in mice. Diabetes 2010;59:1171–1181
36. Murray PJ, Allen JE, Biswas SK, et al. Macrophage activation and polarization: nomenclature and experimental guidelines. Immunity 2014;41:14–20
37. Ito A, Suganami T, Yamauchi A, et al. Role of CC chemokine receptor 2 in bone marrow cells in the recruitment of macrophages into obese adipose tissue. J Biol Chem 2008;283:35715–35723
38. Murray PJ, Wynn TA. Protective and pathogenic functions of macrophage subsets. Nat Rev Immunol 2011;11:723–737
39. Garcia-Martinez I, Santoro N, Chen Y, et al. Hepatocyte mitochondrial DNA drives nonalcoholic steatohepatitis by activation of TLR9. J Clin Invest 2016;126:859–864
40. Nishimoto S, Fukuda D, Higashikuni Y, et al. Obesity-induced DNA released from adipocytes stimulates chronic adipose tissue inflammation and insulin resistance. Sci Adv 2016;2:e1501332
41. Hornung V, Rothenfusser S, Britsch S, et al. Quantitative expression of toll-like receptor 1-10 mRNA in cellular subsets of human peripheral blood

mononuclear cells and sensitivity to CpG oligodeoxynucleotides. J Immunol 2002; 168:4531–4537
42. Lomonaco R, Ortiz-Lopez C, Orsak B, et al. Effect of adipose tissue insulin resistance on metabolic parameters and liver histology in obese patients with nonalcoholic fatty liver disease. Hepatology 2012;55:1389–1397
43. Tan BK, Chen J, Farhatullah S, et al. Insulin and metformin regulate circulating and adipose tissue chemerin. Diabetes 2009;58:1971–1977
44. Stefanovic-Racic M, Yang X, Turner MS, et al. Dendritic cells promote macrophage infiltration and comprise a substantial proportion of obesity-associated increases in CD11c$^+$ cells in adipose tissue and liver. Diabetes 2012;61: 2330–2339
45. Bertola A, Ciucci T, Rousseau D, et al. Identification of adipose tissue dendritic cells correlated with obesity-associated insulin-resistance and inducing Th17 responses in mice and patients. Diabetes 2012;61:2238–2247
46. Song F, Hurtado del Pozo C, Rosario R, et al. RAGE regulates the metabolic and inflammatory response to high-fat feeding in mice. Diabetes 2014;63:1948–1965
47. Blanco P, Palucka AK, Gill M, Pascual V, Banchereau J. Induction of dendritic cell differentiation by IFN-alpha in systemic lupus erythematosus. Science 2001;294:1540–1543
48. Braun D, Caramalho I, Demengeot J. IFN-alpha/beta enhances BCR-dependent B cell responses. Int Immunol 2002;14:411–419
49. Patsouris D, Li PP, Thapar D, Chapman J, Olefsky JM, Neels JG. Ablation of CD11c-positive cells normalizes insulin sensitivity in obese insulin resistant animals. Cell Metab 2008;8:301–309
50. Lackey DE, Olefsky JM. Regulation of metabolism by the innate immune system. Nat Rev Endocrinol 2016;12:15–28
51. Zúñiga LA, Shen WJ, Joyce-Shaikh B, et al. IL-17 regulates adipogenesis, glucose homeostasis, and obesity. J Immunol 2010;185:6947–6959
52. Nishimura S, Manabe I, Nagasaki M, et al. CD8$^+$ effector T cells contribute to macrophage recruitment and adipose tissue inflammation in obesity. Nat Med 2009;15:914–920
53. Wensveen FM, Jelenčić V, Valentić S, et al. NK cells link obesity-induced adipose stress to inflammation and insulin resistance. Nat Immunol 2015;16: 376–385
54. Lee BC, Kim MS, Pae M, et al. Adipose natural killer cells regulate adipose tissue macrophages to promote insulin resistance in obesity. Cell Metab 2016; 23:685–698
55. Martinez J, Huang X, Yang Y. Direct action of type I IFN on NK cells is required for their activation in response to vaccinia viral infection in vivo. J Immunol 2008;180:1592–1597
56. Swann JB, Hayakawa Y, Zerafa N, et al. Type I IFN contributes to NK cell homeostasis, activation, and antitumor function. J Immunol 2007;178:7540–7549
57. Long EO, Kim HS, Liu D, Peterson ME, Rajagopalan S. Controlling natural killer cell responses: integration of signals for activation and inhibition. Annu Rev Immunol 2013;31:227–258
58. Madera S, Rapp M, Firth MA, Beilke JN, Lanier LL, Sun JC. Type I IFN promotes NK cell expansion during viral infection by protecting NK cells against fratricide. J Exp Med 2016;213:225–233
59. Koivisto VA, Pelkonen R, Cantell K. Effect of interferon on glucose tolerance and insulin sensitivity. Diabetes 1989;38:641–647
60. Campbell S, Mclaren EH, Danesh BJ. Rapidly reversible increase in insulin requirement with interferon. BMJ 1996;313:92
61. Muraishi K, Sasaki Y, Kato T, Inada C, Tajiri Y, Yamada K. Classification and characteristics of interferon-related diabetes mellitus in Japan. Hepatol Res 2011; 41:184–188
62. Honda K, Yanai H, Negishi H, et al. IRF-7 is the master regulator of type-I interferon-dependent immune responses. Nature 2005;434:772–777
63. Wang XA, Zhang R, Zhang S, et al. Interferon regulatory factor 7 deficiency prevents diet-induced obesity and insulin resistance. Am J Physiol Endocrinol Metab 2013;305:E485–E495
64. Parker B, Bruce I. SLE and metabolic syndrome. Lupus 2013;22:1259–1266
65. Gyldenløve M, Storgaard H, Holst JJ, Vilsbøll T, Knop FK, Skov L. Patients with psoriasis are insulin resistant. J Am Acad Dermatol 2015;72:599–605
66. Mercer E, Rekedal L, Garg R, Lu B, Massarotti EM, Solomon DH. Hydroxychloroquine improves insulin sensitivity in obese non-diabetic individuals. Arthritis Res Ther 2012;14:R135
67. Wasko MC, McClure CK, Kelsey SF, Huber K, Orchard T, Toledo FG. Anti-diabetogenic effects of hydroxychloroquine on insulin sensitivity and beta cell function: a randomised trial. Diabetologia 2015;58:2336–2343
68. Macfarlane DE, Manzel L. Antagonism of immunostimulatory CpG-oligodeoxynucleotides by quinacrine, chloroquine, and structurally related compounds. J Immunol 1998;160:1122–1131
69. Kuznik A, Bencina M, Svajger U, Jeras M, Rozman B, Jerala R. Mechanism of endosomal TLR inhibition by antimalarial drugs and imidazoquinolines. J Immunol 2011;186:4794–4804
70. Franceschini L, Realdon S, Marcolongo M, Mirandola S, Bortoletto G, Alberti A. Reciprocal interference between insulin and interferon-alpha signaling in hepatic cells: a vicious circle of clinical significance? Hepatology 2011;54:484–494
71. Merrill JT, Wallace DJ, Petri M, et al.; Lupus Interferon Skin Activity (LISA) Study Investigators. Safety profile and clinical activity of sifalimumab, a fully human anti-interferon α monoclonal antibody, in systemic lupus erythematosus: a phase I, multicentre, double-blind randomised study. Ann Rheum Dis 2011;70: 1905–1913
72. Higgs BW, Zhu W, Morehouse C, et al. A phase 1b clinical trial evaluating sifalimumab, an anti-IFN-α monoclonal antibody, shows target neutralisation of a type I IFN signature in blood of dermatomyositis and polymyositis patients. Ann Rheum Dis 2014;73:256–262